Symmetry Protected Topological Phases in One-Dimensional Systems

Frank Pollmann
Max-Planck-Institut für Physik komplexer Systeme, 01187 Dresden, Germany

OXFORD
UNIVERSITY PRESS

Contents

1
Introduction

Classifying and understanding different phases of matter is an important task of condensed matter physics. The class of "conventional" *symmetry broken* phases is well understood in terms of Landau's theory [1]. A paradigmatic example is the $\mathbb{Z}_2$ symmetric Ising model with a symmetric (paramagnetic) and a symmetry broken (ferromagnet) phase. The two phases can be distinct by measuring the magnetization as a *local order parameter*. In contrast, *topological phases* of matter [2] are less understood and no complete classification is known so far. In these notes we are interested in finding schemes that allow us to understand and characterize certain topological phases of matter. Throughout, we consider systems that are described by *local Hamiltonians* (i.e., $H = \sum_n h_n$ with h_n acting on sites near n).

Gapped quantum phases of matter (i.e., phases in which the ground state is separated from the excitation continuum by a finite energy gap) can be very generally defined in terms of local unitary (LU) transformations [3,4]. These LU transformation correspond to applying a finite number of unitary operators that only act locally on the wave function. We say that two gapped ground states are in the same phase if and only if they can be transformed into each other by LU transformations. Alternatively, we can use the definition that two ground states are in the same phase if they are connected adiabatically to each other by a continuous parameter in the Hamiltonian. Using this definition, all states that differ from "trivial" product states only by local fluctuations, i.e., short ranged entanglement (SRE) states, are in the same phase. States that contain non-local quantum correlation, so-called *topologically ordered* states like quantum Hall states or gapped spin liquids, exhibit long-range (LRE) entanglement that cannot be removed by LU transformations. Using this definition, there exists one trivial (SRE) phase and various different topologically ordered phases that differ in terms of their LRE from each other. In one-dimensional (1D) bosonic systems all gapped ground states have only SRE [4].

Once symmetries are imposed, a much richer variety of phases emerges. In terms of the LU transformations this means that when respecting the imposed symmetry, not all SRE states are in the same phase. One class of states falling into this category are the symmetry breaking states discussed above (e.g., the Ising ferromagnet). Another recently discovered class are *symmetry-protected topological* (SPT) phases [5–10]. The defining property of SPT phases is that they do not break a particular symmetry, however, given a certain symmetry constrains, they cannot be adiabatically connected to a trivial product state. Examples of SPT phases include topological insulators [11] which can be protected by time reversal symmetry. For free fermions, SPT phases are classified in the periodic table for topological insulators and superconductors [12, 13].

Another example is the Haldane phase [14,15] in 1D, which is protected by either time reversal, bond-centered inversion, or the dihedral group of the spin rotations [6].

The main focus of these lecture notes lies on SPT phases in 1D bosonic systems. Based on the entanglement properties of 1D systems, we motivate the matrix-product state (MPS) representation of ground states. Using the MPS framework, we will then demonstrate how SPT phases can be classified using projective representations of the symmetries. As a concrete example, we will consider a spin-1 chain described by the Hamiltonian

$$H = J \sum_j \vec{S}_j \cdot \vec{S}_{j+1} + D \sum_j (S_j^z)^2. \tag{1.1}$$

The first term is the standard spin-1 Heisenberg model with antiferromagnetic exchange interactions. The spin-1 Heisenberg model has a gapped ground state that does not break any symmetries [14, 16] (i.e., it is in the Haldane phase). The second term represents a uniaxial single-ion anisotropy. As the parameter $D \geq 0$ is tuned, the system undergoes a phase transition between two gapped phases at $D \approx 1$ [17–19]. In both phases the ground state has the full symmetry of the Hamiltonian! Thus the phase transition cannot be understood in terms of spontaneous symmetry breaking. With the framework developed in these lectures notes, we will be able to distinguish the two phases in terms of a topological invariant and identify the Haldane phase as an SPT phase. Furthermore, we will discuss non-local order parameters that will allow us two detect the two symmetric phases in numerical simulations.

These notes are structures as follows: In Chapter 2 we start by deriving some basic concepts of entanglement including its definition and the area law. We then introduce matrix-product states (MPS) and show that these describe efficiently gapped ground states in 1D. Based on symmetry transformations of MPS we introduce in Chapter 3 the concept of SPT phases. Using an intuitive approach by studying the symmetry transformations of a segment of consecutive site, we demonstrate the stability of SPT phases. In chapter 4 we propose non-local order parameters to detect SPT phases in numerical simulations. We conclude the lecture by summarizing the main result and give a short outlook in Chapter 5.

2
Entanglement and Matrix Product States

Entanglement is one of the fundamental phenomena in quantum mechanics and implies that different degrees of freedom of a quantum system cannot be described independently. Over the past decades it was realized that the entanglement in quantum many-body system can give access to a lot of useful information about quantum states. First, entanglement related quantities provide powerful tools to extract universal properties of quantum states. For example, scaling properties of the entanglement entropy help to characterize critical systems [20–23], and entanglement is the basis for the classification of topological orders [24, 25]. Second, the understanding of entanglement helped to develop new numerical methods to efficiently simulate quantum many-body systems [26, 27]. In the following, we give a short introduction to entanglement in 1D systems and then focus on the MPS representation.

2.1 Schmidt decomposition and entanglement

Let us consider the bipartition of the Hilbert space $\mathcal{H} = \mathcal{H}_L \otimes \mathcal{H}_R$ of a 1D system as illustrated in Fig. 2.1(a), where $\mathcal{H}_L$ ($\mathcal{H}_R$) describes all the states defined on the left (right) of a given bond. In the so called *Schmidt decomposition*, a state $|\Psi\rangle \in \mathcal{H}$ is decomposed as

$$|\Psi\rangle = \sum_\alpha \Lambda_\alpha |\alpha\rangle_L \otimes |\alpha\rangle_R, \quad |\alpha\rangle_{L(R)} \in \mathcal{H}_{L(R)}, \tag{2.1}$$

where the states $\{|\alpha\rangle_{L(R)}\}$ form an orthogonal basis of $\mathcal{H}_L$ ($\mathcal{H}_R$) and $\Lambda_\alpha \geq 0$. The Schmidt decomposition is unique up to degeneracies and for a normalized state $|\Psi\rangle$ we find that $\sum_\alpha \Lambda_\alpha^2 = 1$.

An important aspect is that the Schmidt decomposition gives direct insight into the *bipartite entanglement* (i.e., the entanglement between degrees of freedom in $\mathcal{H}_L$ and $\mathcal{H}_R$) of a state. In particular, only one term contributes to the Schmidt decomposition if and only if L and R are not entangled. If more than one term is required in the Schmidt decomposition to express the state, the state is necessarily entangled. The relation between the Schmidt decomposition and the entanglement can be made more concrete. The *reduced density matrix*

$$\rho^R = \mathrm{Tr}_L \left(|\psi\rangle\langle\psi| \right) \tag{2.2}$$

has the Schmidt states $|\alpha\rangle_R$ as eigenstates and the Schmidt coefficients are the square roots of the corresponding eigenvalues, i.e., $\rho^R = \sum_\alpha \Lambda_\alpha^2 |\alpha\rangle_R\langle\alpha|_R$ (equivalently for

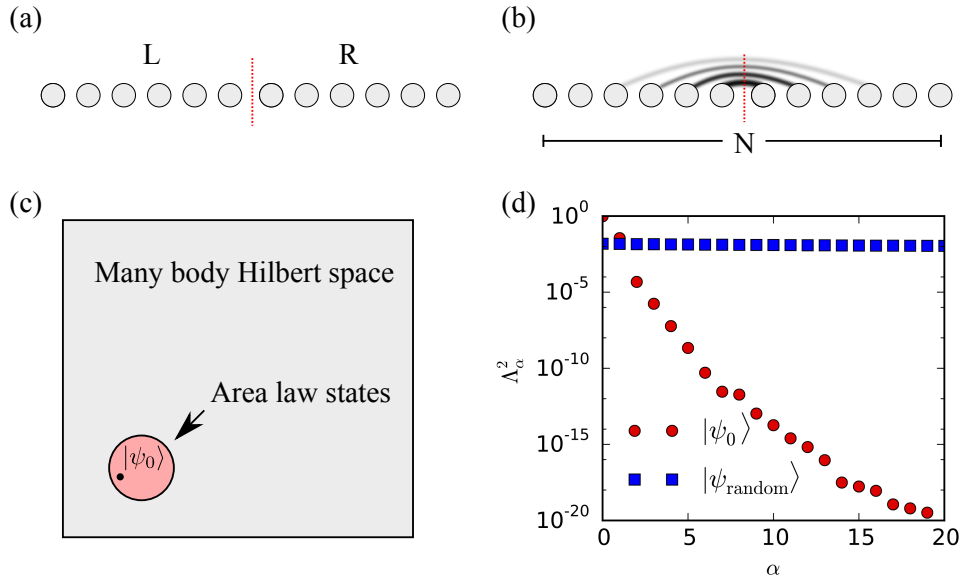

Fig. 2.1 (a): Bipartition of a 1D system into two half chains. (b): Significant quantum fluctuations in gapped ground states occur only on short length scales. (c): 1D area law states make up a very small fraction of the many-body Hilbert space but contain all gapped ground states. (d): Comparison of the entanglement spectrum of the ground state of the transverse field Ising model ($g = 1.5$) and a random state for a system consisting of $N = 16$ spins.

ρ^L). The reduced density matrix of an entangled (pure) quantum state is the density matrix of a mixed state defined on the subsystem. Thus the *entanglement entropy*, which is defined as the von-Neumann entropy of the reduced density matrix, measures the amount of entanglement. In terms of the Schmidt values, it is given by

$$S = -\sum_\alpha \Lambda_\alpha^2 \log \Lambda_\alpha^2. \tag{2.3}$$

The entanglement entropy S is a very useful measure to quantify the amount of entanglement in a system for a given bipartition. Finally, the *entanglement spectrum* $\{\epsilon_\alpha\}$ [28] is defined in terms of the spectrum $\{\Lambda_\alpha^2\}$ of the reduced density matrix by $\Lambda_\alpha^2 = \exp(-\epsilon_\alpha)$ for each α.

2.2 Area Law

A "typical" state in the Hilbert space shows a *volume law*, i.e., the entanglement entropy grows proportionally with the volume of the partitions. In particular, it has been shown in Ref. [29] that a randomly drawn state $|\psi_{\text{random}}\rangle$ from the Hilbert space of a system of N sites with on-site Hilbert space dimension d has an entanglement entropy of $S \approx N/2 \log d - 1/2$ for a bipartition into two parts of $N/2$ sites.

Ground states $|\psi_0\rangle$ of gapped and local Hamiltonians follow instead an *area law*, i.e., the entanglement entropy grows proportionally with the area of the cut [30]. For a cut of an N-site chain as shown in Fig. 2.1(a) this implies that $S(N)$ is constant for $N \gtrsim \xi$ (with ξ being the correlation length). This can be intuitively understood from the fact that a gapped ground state contains only fluctuations within the correlations length ξ and thus only degrees of freedom near the cut are entangled as schematically indicated in Fig. 2.1(b). A rigorous proof of the area law in 1D is given in Ref. [31]. In this respect, ground states are very special states and can be found within a very small corner of the Hilbert space as illustrated in Fig. 2.1(c).

In slightly entangled states, only a relatively small number of Schmidt states contribute significantly. This is demonstrated in Fig. 2.1(d) by comparing the largest 20 Schmidt values of an area law and a volume law state for a bipartition of an $N = 16$ chain into two half chains.

As an example of an area law state, we consider here the ground state of the transverse field Ising model

$$H = -\sum_n \sigma_n^z \sigma_{n+1}^z + g\sigma_n^x, \tag{2.4}$$

with σ_n^x and σ_n^z being the Pauli operators and $g > 0$. The $\mathbb{Z}_2$ symmetric model with a phase transition at $g = 1$ has two very simple limits. For $g = 0$, the ground state is twofold degenerate and given by the ferromagnetic product state (symmetry broken) and at $g \to \infty$, the ground state is a product state in which all spins are polarized (symmetric). For intermediate values of g, the ground states are area law type entangled states (except at the critical point). As shown in Fig. 2.1(d) for a representative example of $g = 1.5$, the ground state has essentially the entire weight contained in a few Schmidt states. Generic states fulfilling the area law show a similar behavior and thus the above observation provides an extremely useful approach to compress quantum states by truncating the Schmidt decomposition. In particular, we can always truncate the Schmidt decomposition at some finite χ such that

$$\left\| |\psi\rangle - \sum_{\alpha=1}^{\chi} \Lambda_\alpha |\alpha\rangle_L \otimes |\alpha\rangle_R | \right\| < \epsilon, \quad \forall \epsilon > 0. \tag{2.5}$$

This particular property of area law states is intimately related to the MPS representation of 1D quantum states as we will demonstrate in the next section.

The situation is very different for a highly entangled (volume law) random state: All the Schmidt values are roughly constant for all $2^{N/2}$ states and thus only little weight in contained in the 20 dominant states (assuming an equal weight, we find $\sim 1/2^{N/2}$ per Schmidt state).

2.3 Matrix Product States

A generic quantum state $|\Psi\rangle$ on a chain with N sites can be written in the following MPS form [32–34]:

$$|\Psi\rangle = \sum_{j_1,\ldots,j_N} A^{[1]j_1} A^{[2]j_2} \ldots A^{[N]j_N} |j_1, \ldots, j_N\rangle. \tag{2.6}$$

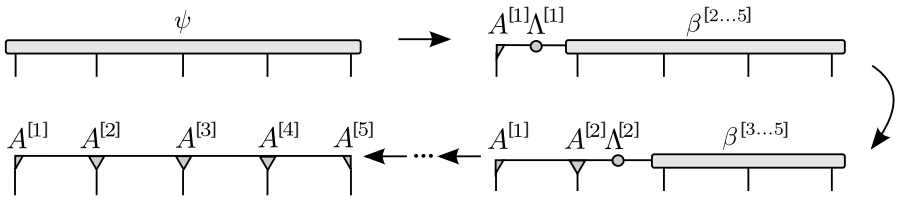

Fig. 2.2 Iterative conversion of a state $|\psi\rangle$ given by a rank-N tensor $\psi_{i_1,\ldots,i_N}$ using successive Schmidt decompositions in a diagrammatic representations. The horizontal lines represent the bond (Schmidt indices) $\alpha, \beta, \gamma, \ldots$ and the vertical lines the physical indices $j_n \in \{1, \ldots, d\}$. Connected lines between tensors denote summation over the corresponding indices (see text for details).

Here, $A^{[n]j_n}$ is a $\chi_{n-1} \times \chi_n$ dimensional matrix and $|j_n\rangle$ with $j_n = 1, \ldots, d$ is a basis of local states at site n. We call the indices of the matrices "bond" indices. The matrices at the boundary, i.e., $n = 1$ and $n = N$, are vectors, that is $\chi_0 = \chi_N = 1$, such that the matrix product in Eq. Eq. (2.6) produces a number. The superscript $[n]$ denotes the fact that for a generic state, each site is represented by a different set of matrices.

In order to provide some intuition for the structure of MPS, we demonstrate how to transform a generic quantum state

$$|\psi\rangle = \sum_{j_1, j_2, \ldots, j_N} \psi_{j_1, j_2, \ldots, j_N} |j_1, j_2, \ldots j_N\rangle \tag{2.7}$$

into an MPS. This can be done exactly by performing successively Schmidt decompositions as shown diagrammatically in Fig. 2.2. This diagrammatic representation, in which a rank-N tensor is represented by a symbol with N legs, is very useful for representing tensor networks and related algorithms. Connecting the legs among tensors symbolizes a tensor contraction, i.e., summing over the relevant indices.

We start by performing a Schmidt decomposition Eq. (2.1) of the state $|\psi\rangle$ into the first site and the rest such that

$$|\psi\rangle = \sum_{\alpha_1=1}^{d} \Lambda^{[1]}_{\alpha_1} |\alpha_1\rangle_{[1]} |\alpha_1\rangle_{[2,\ldots,N]}. \tag{2.8}$$

The states $|\alpha_1\rangle_{[1]}$ and $|\alpha_1\rangle_{[2,\ldots,N]}$ form an orthogonal basis for the left and right part, respectively. The first matrix $A^{[i]j_1}_{\alpha_1}$ in the MPS is the matrix relating the left Schmidt states $|\alpha_1\rangle_{[1]}$ with the local states $|j_1\rangle$ (describing the local states on the first site) and is given by $A^{[1]j_1}_{\alpha_1} = \langle j_1|\alpha_1\rangle_{[1]}$. The resulting mixed representation of the state reads

$$|\psi\rangle = \sum_{j_1=1}^{d} \sum_{\alpha_1=1}^{d} A^{[1]j_1}_{\alpha_1} \Lambda^{[1]}_{\alpha_1} |j_1\rangle |\alpha_1\rangle_{[2,\ldots N]}. \tag{2.9}$$

Next we proceed to the next bond and perform a Schmidt decomposition of the state such that

$$|\psi\rangle = \sum_{\alpha_2=1}^{d^2} \Lambda^{[2]}_{\alpha_2} |\alpha_2\rangle_{[1,2]} |\alpha_2\rangle_{[3,\ldots,N]}. \tag{2.10}$$

The second matrix $A^{[2]j_2}_{\alpha_1\alpha_2}$ then relates the mixed basis states $|\alpha_1\rangle_{[1]}|j_2\rangle$ with the left Schmidt states $|\alpha_2\rangle_{[1,2]}$ and is given by $A^{[2]j_2}_{\alpha_1\alpha_2} = \left[\langle\alpha_1|_{[1]}\langle j_2|\right]|\alpha_2\rangle_{[1,2]}$. The resulting mixed representation of the state reads

$$|\psi\rangle = \sum_{\alpha_1=1}^{d} \sum_{\alpha_2=1}^{d^2} \sum_{j_1,j_2=1}^{d} A^{[1]j_1}_{\alpha_1} A^{[2]j_2}_{\alpha_1\alpha_2} \Lambda^{[2]}_{\alpha_2} |j_1, j_2\rangle |\alpha_2\rangle_{[3,\ldots,N]}. \tag{2.11}$$

This procedure can now be continued until reaching the right end of the chain. We choose the last matrix $A^{[N]j_n}$ to relate the states $\Lambda_{\alpha_N}|\alpha_n\rangle_{[N]}$ to the local basis $|j_n\rangle$. Then it is easy to see that we finally arrive at a representation of the state that has exactly the form Eq. (2.6).

The caveat is that the matrix dimension increases exponentially as we proceed toward the center of the chain. However, we can make an approximation by neglecting the Schmidt states that have a very small Schmidt values. For the ground state of the Ising model discussed above, we can find a very good approximation of the ground state as MPS by keeping only a maximal bond dimension of $\sim$20 with a truncation error that is of the order of the machine precision (independent of the system size). The same picture can be generalized to all states that fulfill an area law. On more general grounds it had been proven that ground states of one dimensional gapped systems can be efficiently approximated by an MPS [35, 36].

2.3.1 Canonical form

The representation Eq. (2.6) is not unique as an MPS with the transformed matrices

$$\tilde{A}^{[n]i_n} = X_{n-1} A^{[n]i_n} X_n^{-1} \tag{2.12}$$

represents the same state, where the X_n are $\chi_n \times \chi_n$ matrices. In the following, we will show how to fix this degree of freedom by introducing a convenient *canonical* form of the MPS in which the bond index corresponds to the Schmidt decomposition.

Without a loss of generality, we write the matrices $A^{[n]j_n}$ as a product of $\chi_{j-1} \times \chi_j$ complex matrices $\Gamma^{[n]j_n}$ and positive, real, square diagonal matrices $\Lambda^{[n]}$,

$$|\Psi\rangle = \sum_{j_1,\ldots,j_N} \Gamma^{[1]j_1} \Lambda^{[1]} \Gamma^{[2]j_2} \Lambda^{[2]} \ldots \Lambda^{[N-1]} \Gamma^{[N]j_N} |j_1, \ldots, j_N\rangle, \tag{2.13}$$

as pictorially illustrated in Figs. 2.3(a) and 2.3(b). Let us now motivate the particular choice Eq. (2.13) for the MPS form. The freedom of choosing the MPS can be used to define a "canonical form" of the MPS, following Ref. [37, 38]. As we will see later on, the canonical form has several very useful features. Any bond n defines a bipartition of the system into sites $L = \{1, \ldots, n\}$ and $R = \{n+1, \ldots, N\}$ to the left and right of the bond. From the form of the MPS, we can define a set of χ_n wave functions

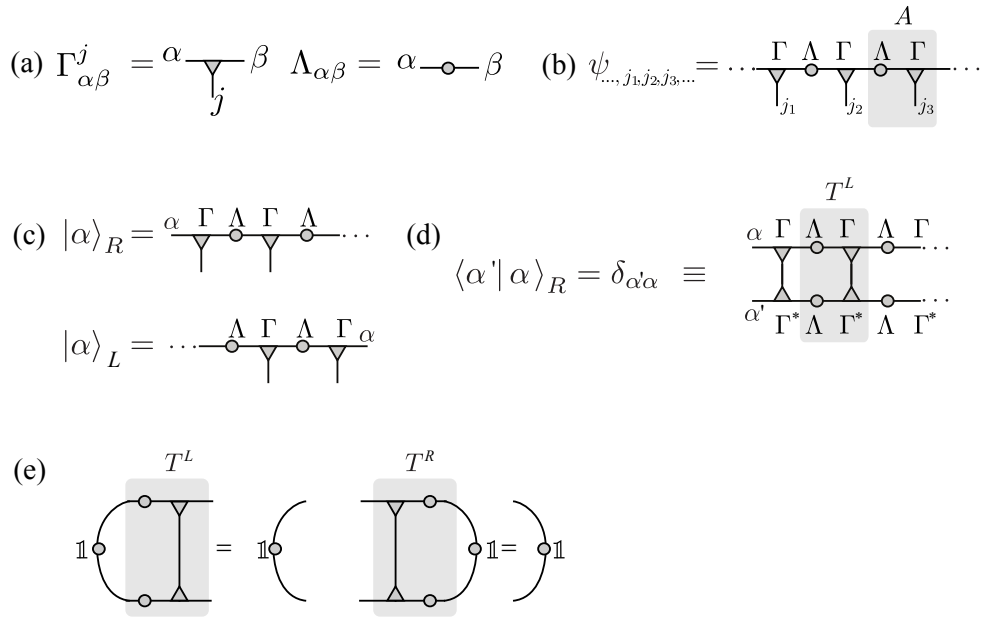

Fig. 2.3 (a): Diagrammatic representation of the tensors Γ and Λ. (b): MPS formed by the tensors Γ and Λ. (c): Definition of the right Schmidt basis states with respect to a partition on a bond with index α. (d): Condition for the MPS to be in the canonical form. The transfer matrix T^L of Eq. (2.16) has been shaded. The upside-down triangles are the complex conjugate of the Γ tensors. (e): If the state is in canonical form, then the dominant left eigenvector of T^L is the "identity matrix" with eigenvalue equal to 1. A similar condition applies for the right transfer matrix T^R.

$|\alpha\rangle_{[1,\ldots,n]}$ and $|\alpha\rangle_{[n+1,\ldots,N]}$ to the left/right of the bond [see Fig. 2.3(c)] such that state takes the form

$$|\psi\rangle = \textstyle\sum_{\alpha=1}^{\chi} \Lambda_\alpha^{[n]} |\alpha\rangle_{[1,\ldots,n]} \otimes |\alpha\rangle_{[n+1,\ldots,N]}. \tag{2.14}$$

The wave functions $|\alpha\rangle_{L/R}$ are formed by multiplying all matrices to the left and right, respectively. The MPS representation $\{\Gamma^{[1]}, \Lambda^{[1]}, \ldots, \Gamma^{[N]}\}$ is in canonical form if: *For every bond, the set of Schmidt states along with* $\Lambda^{[n]}$ *form a Schmidt decomposition of* Ψ. In other words we must have $\langle\alpha'|\alpha\rangle_{[1,\ldots,n]} = \delta_{\alpha'\alpha}$ and $\langle\alpha'|\alpha\rangle_{[n+1,\ldots N]} = \delta_{\alpha'\alpha}$, along with $\sum(\Lambda_\alpha^{[n]})^2 = 1$ on every bond. For finite systems, a generic MPS can be transformed into canonical form by successively orthogonalizing the bonds starting from either the left or right end of the chain [27]. A great advantage of the canonical form is that local expectation values can be evaluated by only contracting the tensors locally by using the orthogonality. Note that the MPS form we obtained above by applying successively Schmidt decomposition provides naturally the canonical form with $A^{[n]j_n} = \Lambda^{[n-1]}\Gamma^{[n]j_n}$.

2.3.2 Infinite matrix product states

For infinite ($N \to \infty$) and translationally invariant systems, the set of matrices on any given site becomes the same, that is $\Gamma^{[n]j} = \Gamma^j$ and $\Lambda^{[n]} = \Lambda$ for all integers n. Computing the overlaps $\langle\alpha'|\alpha\rangle_R$ would appear to require an infinite tensor contraction. For an infinite MPS, the orthogonality condition can be conveniently expressed in terms of the *transfer matrix* T^R [illustrated in Fig. 2.3(d)] defined as

$$T^R_{\alpha\alpha';\beta\beta'} = \sum_j \Gamma^j_{\alpha\beta} \left(\Gamma^j_{\alpha'\beta'}\right)^* \Lambda_\beta \Lambda_{\beta'}, \tag{2.15}$$

where "*" denotes complex conjugation [38]. The transfer matrix T^R relates the overlaps defined on bond n with overlaps defined on bond $n+1$. Given that the right basis states $|\beta\rangle_R^{[n+1]}$ on bond $n+1$ are orthonormal, the states $|\alpha\rangle_R^{[n]}$ on bond n will also be orthonormal if T has a dominant *right* eigenvector $\delta_{\beta\beta'}(= \mathbb{1})$ with eigenvalue $\eta = 1$, as illustrated in Fig. 2.3(e). For the left set of states we define an analogous transfer matrix T^L,

$$T^L_{\alpha\alpha';\beta\beta'} = \sum_j \Lambda_\alpha \Lambda_{\alpha'} \Gamma^j_{\alpha\beta} \left(\Gamma^j_{\alpha'\beta'}\right)^* \tag{2.16}$$

which must have a *left* eigenvector $\delta_{\alpha\alpha'}$ with $\eta = 1$. These eigenvector criteria are clearly necessary conditions for all bonds to be canonical; in fact, assuming in addition that $\eta = 1$ is the dominant eigenvalue, they are sufficient.

A state is called *pure* if the dominant eigenvalue is unique and *mixed* if it is degenerate. In the following discussions, we will always assume that the state is *pure* (in fact every mixed state can be uniquely decomposed into pure ones). An algorithm to explicitly transform an arbitrary infinite MPS to the canonical form involves diagonalizing the two transfer matrices T^R and T^L and is given in Ref. [39]. If the infinite MPS is not translational invariant with respect to a one-site unit cell, all the above can be simply generalized by considering a unit-cell of L sites which repeats itself, e.g., in the case of a two site unit cel, the tensors are given by

$$\begin{aligned} \Gamma^{[2n]} &= \Gamma^A, & \Lambda^{[2n]} &= \Lambda^A, \\ \Gamma^{[2n+1]} &= \Gamma^B, & \Lambda^{[2n+1]} &= \Lambda^B, \end{aligned} \tag{2.17}$$

for $n \in \mathbb{Z}$. Reviews of MPSs as well as the canonical form can be found in Refs. [40, 39, 38].

The infinite MPS representation in the canonical form has a number of important advantages. First, using the properties of the transfer matrices [Fig. 2.3(e)], it is very convenient to evaluate local expectation values as well as correlation functions. Second, with the help of efficient algorithms such as the *infinite time evolving block decimation* (iTEBD) [38] or *infinite density matrix renormalization group method* (iDMRG) [41], the ground state of a given Hamiltonian can be found in the thermodynamic limit. A discussion of the two algorithms using the same notation as used in these notes can be found in Ref. [42].

2.3.3 Examples of infinite MPS

To become more familiar with the infinite MPS representation, it is instructive to consider a few concrete examples.

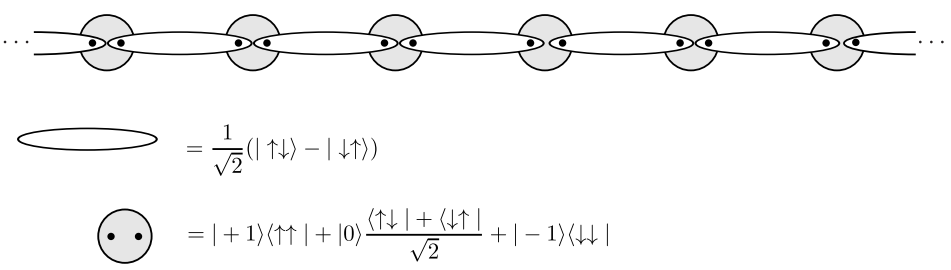

Fig. 2.4 Diagrammatic representation of the AKLT states. The $S = 1$ sites (grey circles) are decomposed into two $S = 1/2$ that are forming a singlet with the neighboring site (ellipsoids).

(1) Neel state. The state $|\ldots\uparrow\downarrow\uparrow\downarrow\ldots\rangle$ is a product state with a bond dimension $\chi = 1$ and a local Hilbert space of $d = 2$. The infinite MPS representation is given by

$$\begin{aligned}\Gamma^{[2n],\uparrow} &= \Gamma^{[2n+1],\downarrow} = 1\\ \Gamma^{[2n],\downarrow} &= \Gamma^{[2n+1],\uparrow} = 0\\ \Lambda^{[2n]} &= \Lambda^{[2n+1]} = 1.\end{aligned}$$

Note that since the state is a simple product state, the matrices are actually simply complex numbers. It is easy to see that a contraction of the infinite MPS yields the desired Neel state. Furthermore, the corresponding transfer matrices trivially obey the conditions for the canonical form.

(2) Spin-1 AKLT state. Affleck, Kennedy, Lieb, and Tasaki (AKLT) constructed an $S = 1$ Hamiltonian for which the ground state has valence bonds between all neighboring sites (see Fig. 2.4) [43]. The AKLT Hamiltonian consists of a sum of projectors and reads

$$H = \sum_j \vec{S}_j \vec{S}_{j+1} + \frac{1}{3}(\vec{S}_j \vec{S}_{j+1})^2, \tag{2.18}$$

where $\vec{S}$ are the spin-1 operators. The ground state in the thermodynamic limit is unique and has a simple ($\chi = 2$) infinite MPS representation

$$\Gamma^{[n],-1} = \sqrt{\frac{4}{3}}\sigma^+,\ \Gamma^{[n],0} = -\sqrt{\frac{2}{3}}\sigma^z,\ \Gamma^{[n],1} = -\sqrt{\frac{4}{3}}\sigma^- \tag{2.19}$$

$$\Lambda^{[n]} = \sqrt{\frac{1}{2}}\begin{pmatrix}1 & 0\\ 0 & 1\end{pmatrix}. \tag{2.20}$$

The state can be shown to be in the canonical form by diagonalizing the corresponding left and right transfer matrices.

3

Symmetry Protected Topological Phases

3.1 Symmetry transformations of Matrix-Product States

For the study of SPT phases, it will be essential to understand how symmetry operations act on MPS. Let us consider an on-site symmetry operation which is applied to all sites, i.e.,

$$|\tilde{\psi}\rangle = \left[\bigotimes_n u_n(g)\right] |\psi\rangle, \tag{3.1}$$

where $u_n(g)$ is acting on site n with g being an element of the symmetry group G under which the state $|\psi\rangle$ is invariant. An example of such symmetry is the $\mathbb{Z}_2$ symmetry $\bigotimes_n \sigma_n^x$ of the transverse field Ising model Eq. (2.4). In the MPS formulation, the transformation corresponds to contracting the symmetry operation to all physical legs as shown in Fig. 3.1(a). In order for a state to be invariant, the overlap of the original state with the transformed state has to be of modulus one, i.e., $|\langle\tilde{\psi}|\psi\rangle| = 1$. Thus the mixed transfer matrices of the original and the transformed MPS must have a dominant eigenvector X with eigenvalues $|\eta| = 1$. The right mixed transfer matrix has the form

$$T^R_{\alpha\alpha';\beta\beta'}(g) = \sum_n \left(\sum_{n'} u_{nn'}(g)\Gamma^{n'}_{\alpha\beta}\right)\left(\Gamma^{j}_{\alpha'\beta'}\right)^* \Lambda_\beta\Lambda_{\beta'} \tag{3.2}$$

and fulfills

$$\sum_{\beta,\beta'} T^R_{\alpha\alpha';\beta\beta'}(g) X_{\beta\beta'} = \eta X_{\alpha\alpha'}. \tag{3.3}$$

Analogously, we find a similar relation for the left mixed transfermatrix $T^L(g)$. See also the diagrammatic representation in Fig. 3.1(b). If $|\eta| < 1$, the overlap between the original and the transformed wave function decays exponentially with the length of the chain and $|\psi\rangle$ is thus not invariant.

In Ref. [44] it was shown that an MPS in canonical form that the matrices Γ^j transform under symmetry operations g as

$$\sum_{j'} u_{jj'}(g)\Gamma^{j'} = e^{i\theta_g} U^\dagger(g)\Gamma^j U(g), \tag{3.4}$$

with a diagrammatic representation as shown in Fig. 3.1(c). Here $U(g)$ is a unitary matrix which commutes with the Λ matrices, and $e^{i\theta(g)}$ is a phase. [1] It is clear that this

[1] As $U(g)$ commutes with Λ, it also commutes with the reduced density matrices ρ^L and ρ^R.

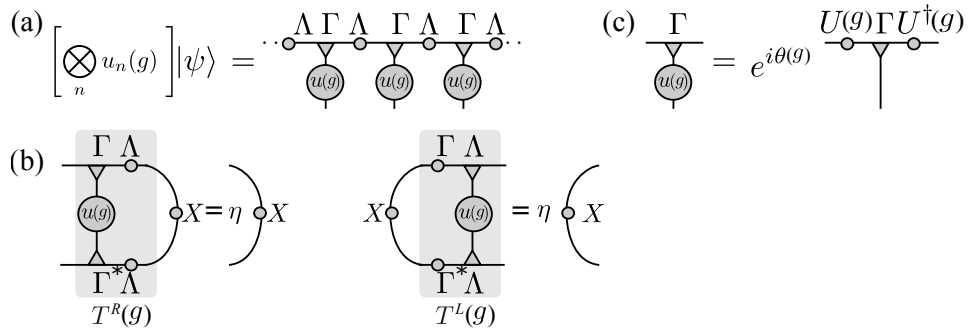

Fig. 3.1 (a): Transformation of an MPS under an on-site symmetry g applied to all sites. (b): Representation of a symmetry operation in terms of the MPS. (c): Mixed transfer matrices of the original and the transformed states.

is a sufficient condition for the mixed transfer matrices to have a dominant eigenvalue of modulus one. To show that it is a necessary condition, one has to apply Schwarz-inequality and use conditions of the canonical form. [44]. The matrices $U(g)$ are form a $\chi-$dimensional *projective* representation of the symmetry group of the wavefunction and $e^{i\theta(g)}$ is a linear (1D) representation [45]. The term projective means that the $U(g)$ are a representation of the symmetry modulo a phase. As discussed in the following sections, the fact that the $U(g)$ can be projective representations of the symmetries are the key to understand SPT phases. Note that the matrices $U(g)$ are actually a representation of the symmetry operations in the basis of Schmidt states (this can be seen by going back to the definition of the canonical form).

Similar relations can be derived for symmetries that are not on-site operations. For a time reversal transformation Γ^j is transformed to $(\Gamma^j)^*$ (complex conjugate) on the left hand side (including possible spin rotations). In the case of inversion symmetry Γ^j is transformed to $(\Gamma^j)^T$ (transpose) on the left hand side of Eq. (3.4). We refer to Ref. [45] for further details.

3.2 Classification of projective representations

Let us assume a group G with group elements $g_i \in G$. Then the matrices $U(g_i)$ form a *projective* representation of G if

$$U(g_i)U(g_j) = \omega(g_i, g_j)U(g_i g_j), \tag{3.5}$$

where $\omega(g_i, g_j) \in U(1)$ represent the so-called *factor set*. Thus a projective representation is a linear representation modulo a $U(1)$ phase factor. In the case that all phase factors are unity, then the representation is a linear representation of the group. Because of the associativity of the group (i.e., the elements of G fulfill $g_i(g_j g_k) = (g_i g_j)g_k$), the factor set must satisfy

$$\omega(g_j, g_k)\omega(g_i, g_j g_k) = \omega(g_i g_j)\omega(g_i g_j, g_k). \tag{3.6}$$

Transforming the matrices as $\tilde{U}(g_i) = \beta(g_i)U(g_i),\ \beta(g_i) \in U(1)$ yields a new factor set

$$\tilde{\omega}(g_i, g_j) = \frac{\beta(g_i g_j)}{\beta(g_i)\beta(g_j)}\omega(g_i, g_j). \tag{3.7}$$

Two projective representations $\tilde{U}(g)$ and $U(g)$ that are related by such a transformation are considered to be equivalent and belong to the same class.

It was Isaac Schur who derived in 1904 a classification of different types of projective representation using so called "Schur multipliers" to label different classes. These correspond to the second cohomology group $H_2(G, U(1))$ of a group G. Instead of discussing the details of the proof, we refer for a general introduction to Ref. [46] and consider some simple examples.

(1) Group $\mathbb{Z}_\mathbb{N}$. The generators of the group are $\exp(i\pi/N)$ rotations and the group elements are $\{1, R, R^2, \ldots, R^N\}$. For a projective representation of the group we can assign an arbitrary phase such that $U^N(R) = \exp(i\phi)$. However, a simple rescaling $U(R)$ by $\exp(i\phi/N)$ can always transform the projective representation to a linear one. Thus this group has only one class and all projective representation can be transformed into a linear one.

(2) Group $\mathbf{D_2}$. This group is generated by π rotations R_x and R_z about two orthogonal axes. Clearly, $R_x^2 = R_z^2 = 1$ and $R_z R_x = R_x R_z$, thus the group elements are $\{1, R_x, R_z, R_x R_z\}$. The group D_2 has two different classes of projective representations which can be distinguished by the gauge invariant phase factor

$$U(R_x)U(R_z)U^{-1}(R_x)U^{-1}(R_z) = \exp(i\phi)$$

with $\phi = 0, \pi$. Clearly, as each element occurs with its inverse, the phase of the commutator cannot be change by rephasing the operators.

Both cases can be realized using a representation of the rotations in terms of spin operators by $U(R_x) = \exp(i\pi S^x)$ and $U(R_z) = \exp(i\pi S^z)$. The $S = 1$ representation with

$$S^x = \frac{1}{\sqrt{2}}\begin{pmatrix} 0 & 1 & 0 \\ 1 & 0 & 1 \\ 0 & 1 & 0 \end{pmatrix}, S^z = \begin{pmatrix} -1 & 0 & 0 \\ 0 & 0 & 0 \\ 0 & 0 & 1 \end{pmatrix}. \tag{3.8}$$

is a linear ($\phi = 0$) representation. The $S = 1/2$ spin matrices

$$S^x = \frac{1}{2}\begin{pmatrix} 0 & 1 \\ 1 & 0 \end{pmatrix}, S^z = \frac{1}{2}\begin{pmatrix} 1 & 0 \\ 0 & -1 \end{pmatrix}. \tag{3.9}$$

form a projective ($\phi = \pi$) representation. This can be seen easily as $U(R_x) = \sigma_x$ and $U(R_z) = \sigma_z$ anti-commute (σ_x, σ_z are the Pauli matrices).

3.3 Symmetry fractionalization

We now come to the core of these notes and define SPT phases in 1D bosonic systems that are protected by an on-site symmetry group G. The classification scheme is based on the classification of projective representations in terms of the second cohomology classes $H_2(G, U(1))$ [6–9]. While the general proof for the existence of SPT phases is given in terms of a classification of fixed point wave functions of LU transformations [7–9], we follow here a more intuitive approach.

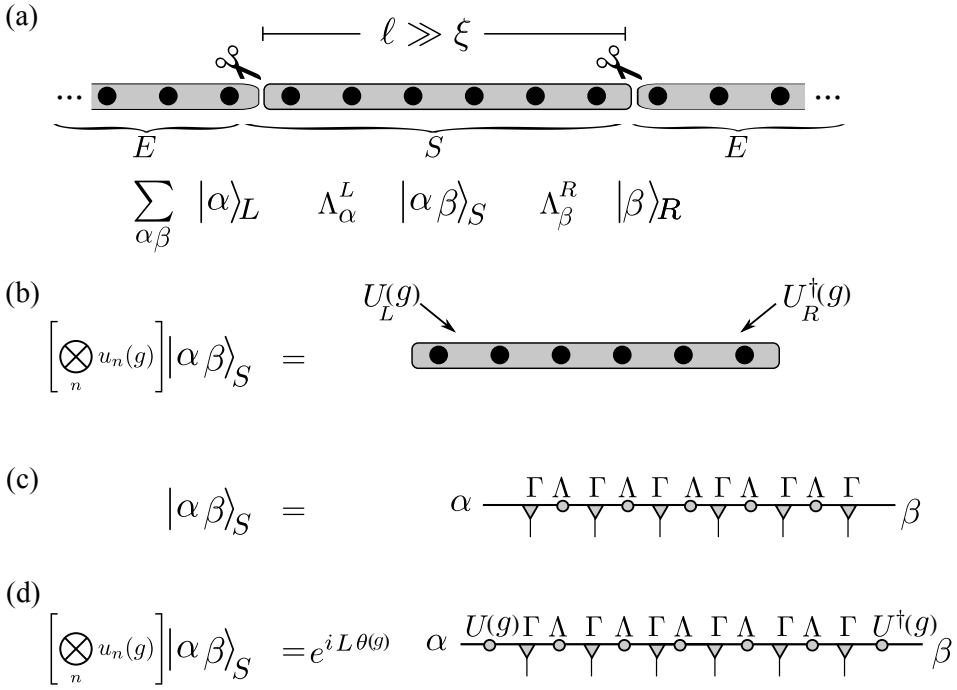

Fig. 3.2 (a): Partition of an infinite quasi-1D system into a segment S and an environment E. The segment S is a finite region of the system chosen to be large compared to the correlation length ξ. The Schmidt states on the segment of a ground state $|\psi_0\rangle$ are decomposed into tensor products of the left (α) and right (β) part. (b): Symmetry operations acting on the dominant Schmidt states of the segment S can be represented in terms of operators acting on the boundaries. (c): Given that $|\psi_0\rangle$ is an infinite MPS formed by the χ dimensional matrices $\{\Gamma^j, \Lambda\}$, then the contraction of the matrices yields the χ^2 dominant Schmidt states on the segment. (d): The Schmidt states on the segment transform under symmetry operation by local unitary transformations acting on the boundaries. These are the (projective) representations of the symmetries as defined in Eq. (3.4).

We consider systems in which the onsite representation is linear (e.g., integer spin systems). We show that a characteristic *symmetry fractionalization* occurs when applying a symmetry operation $g \in G$ to the dominant Schmidt states of a segment S of length $\ell \gg \xi$ that we cut out of the ground state as shown in Fig. 3.2(a) and (b). Using the locality of the ground states, we show that the symmetry operations act only non trivially on the boundary of the segment. We then argue that the representation of the symmetry actions onto the boundaries provides exactly the projective representations $U(g)$ as defined in the preceding sections. As the two boundaries can be arbitrarily far away from each other, the class of the projective representation cannot be changed unless a phase transition occurs. Thus we can use it to define a phase! *We define an*

SPT phase as a phase in which the boundary of the segment transforms projectively under a symmetry operation g while the bulk is in a linear representation. Clearly, if the necessary symmetries are broken, the phase is not longer well defined.

We will now discuss the details of the argument and relate it to the MPS formulation. Starting from a ground state $|\psi_0\rangle$ of a gapped Hamiltonian, we partition the system into regions ESE as shown in Fig. 3.2(a). The Schmidt decomposition for this bipartition is given by

$$|\psi_0\rangle = \sum_\gamma \Lambda_\gamma |\gamma\rangle_E |\gamma\rangle_S. \tag{3.10}$$

Here $|\gamma\rangle_{E/S}$ are the Schmidt states. A crucial point is that if the width ℓ of the segment is large compared to ξ, the fluctuations across the left cut should be *independent* of the fluctuations across the right cut. The resulting Schmidt decomposition has then a tensor product structure for the important (dominant) Schmidt states. Now we label the left, right fluctuations by α and β and replace the Schmidt index γ by the pair $\gamma = (\alpha, \beta)$. Using $\Lambda_\gamma = \Lambda^L_\alpha \Lambda^R_\beta$ and $|\gamma\rangle_E = |\alpha\rangle_L \otimes |\beta\rangle_R$, we have

$$|\psi\rangle = \sum_{\alpha,\beta} \Lambda^L_\alpha \Lambda^R_\beta |\alpha\rangle_L |\alpha\beta\rangle_S |\beta\rangle_R, \tag{3.11}$$

as illustrated in Fig. 3.2(a). In this decomposition, we can think of the indices α/β labeling the local fluctuations at the left/right of the segment. In each Schmidt state $|\alpha\beta\rangle_S$, the expectation values of any local operator has some particular spatial dependence near the ends of the chain depending on α and β, but this decays exponentially to the ground state away from the ends. Therefore it is possible to transform between these states by using operators defined on just the ends. A special case is the effective representations of symmetries in terms of operators $U(g)$ at the ends of the segments as illustrated in Fig. 3.2(b).

The above argument becomes more transparent when representing the states as MPS. With the definition of the canonical form, the states $|\alpha\beta\rangle_S$ of a segment are given by

$$|\alpha\beta\rangle_S = \sum_{\{j_i\}} (\Gamma^{j_1} \Lambda \Gamma^{j_2} \dots \Lambda \Gamma^{j_\ell})_{\alpha\beta} |j_1, j_2, \dots, j_\ell\rangle \tag{3.12}$$

as shown in Fig. 3.2(c). Here we assume that the state $|\psi_0\rangle$ is given as an infinite and translationally invariant MPS. When ℓ is large compared to the correlation length ξ, these states are nearly orthonormal, that is $\langle\alpha'\beta'|_S \alpha\beta\rangle_S \sim \delta_{\alpha'\alpha}\delta_{\beta'\beta}$. In this limit, $|\alpha\beta\rangle_S$ are the Schmidt eigenstates of the segment. If we transform the state using a symmetry operation g, then the matrices transform according to Eq. (3.4). As all unitaries $U(g)$ cancel each other with the bulk, only the ones at the two boundaries remain and we obtain the form shown in Fig. 3.2(d). Now, the two matrices $U(g)$ and $U^\dagger(g)$ are the representations of the symmetry action in terms of the boundaries and thus exactly those we introduced above. The phase factors $e^{i\theta(g)}$ sum up to an overall phase (which characterizes in fact different phases as long as translational invariance is preserved). The class of the projective representation $\{U(g)\}$ of $g \in G$ cannot be changed locally and thus it is "stable" as long as the correlation length remains finite. This is why SPT phases are stable as long as the symmetry is unbroken!

In a closely related way, SPTs can be defined in the presence of symmetries that do not have a simple on-site representation. Examples of symmetries are inversion and time-reversal symmetries and combinations thereof. We refer to the Refs. [45,47,9,7,8] for the details.

Note that the stability relies on the linear on-site representation of the symmetry. If a model allows for local fluctuations of the representations (e.g, by mixing integer and half-integer representations of the spin-rotation symmetry), the SPT phase can be adiabatically connected to a trivial phase [48].

3.4 Spin-1 chain and the Haldane phase

We will now illustrate the main ideas of the classification of SPT by discussing a specific example, namely the spin-1 chain described by the Hamiltonian:

$$H = J \sum_j \vec{S}_j \cdot \vec{S}_{j+1} + D \sum_j (S_j^z)^2. \tag{3.13}$$

As already discussed in the introduction, the first term is the standard spin-1 Heisenberg model with antiferromagnetic exchange interactions which stabilizes the Haldane phase [14,16]. When the single ion anisotropy $D \geq 0$ is tuned, the system undergoes a phase transition between two gapped, *symmetric* phases at $D \approx 1$ [17–19]. The "Haldane" phase at small D is an SPT phase and cannot be adiabatically connected to any product state as long as we preserve either time reversal, bond-centered inversion, or the dihedral group of the spin rotations symmetry [49,6]. It has been shown numerically, that the Haldane phase is adiabatically connected to the AKLT state $|\psi_{\mathrm{AKLT}}\rangle$. The so-called "large D" phase is adiabatically connected to a simple product state

$$|\psi_{\text{large } D}\rangle = \ldots |0\rangle|0\rangle|0\rangle \ldots,$$

which is the ground state of the Hamiltonian for $D \to \infty$. As the phase is adiabatically connected to a simple product state, we refer to the large D phase as trivial phase.

We now use the two simple representatives $|\psi_{\mathrm{AKLT}}\rangle$ and $|\psi_{\text{large D}}\rangle$ to characterize the two phases. Besides many other symmetries, Hamiltonian Eq. (3.13) has a D_2 on-site symmetry. The D_2 symmetry is a subgroup of the $U(1) \rtimes \mathbb{Z}_2$ spin rotation symmetry, namely the Hamiltonian is invariant under rotating all spins continuously about the z axis and π rotations about the x axis. Clearly, the onsite representation of the D_2 in terms of the spin-1 degrees of freedom is a linear one. Let us now analyze how the MPS representation Eq. (2.20) of $|\psi_{\mathrm{AKLT}}\rangle$ transforms under the D_2 symmetry. Using Eq. (3.4) with g_k being the π rotation about the x and z axis, we find that

$$U(R_x) = \sigma_x,\ U(R_z) = \sigma_z$$

and $\theta = \pi$ (To arrive it this result, one can simply apply the on-site symmetry operations to the MPS). The representation of D_2 is a projective one with the gauge invariant phase factor $U(R_x)U(R_z)U^\dagger(R_x)U^\dagger(R_z) = -1$. The MPS representation of

$|\psi_{\text{large D}}\rangle$ is a simple product state of matrices in the $|0\rangle$ state. Thus the MPS transforms trivially under the D_2 rotations

$$U(R_x) = 1,\ U(R_z) = 1$$

with $U(R_x)U(R_z)U^\dagger(R_x)U^\dagger(R_z) = 1$ and $\theta = 0$. As agued above, these phase factors characterize the two phases as they cannot be changed unless the symmetry is broken or the system undergoes a phase transition.

4
Detection

The definitions in the previous section tell us exactly what kind of topological phases exist in 1D bosonic systems and how to classify them. It does, however, not give us a direct method to detect different phases. Here we discuss some practical ideas of how to detect SPT in numerical simulations.

4.1 Degeneracies in the entanglement spectrum

In Ref. [45] it is pointed out that topologically non-trivial phases must have degeneracies in the entanglement spectrum. This is, *all* eigenvalues of the reduced density matrices ρ^L and ρ^R for the bipartition of the system into two half chains are degenerate.

To see this, let us assume that the ground state is represented as an MPS and symmetric under a symmetry group G. Using the Eq. (3.4), we find the symmetry representation $U(g)$ in terms of the auxiliary indices which commutes with the reduced density matrices. If the $U(g)$ for $g \in G$ form a projective representation of the symmetry group, we can find a set of non-commuting elements such that for example $U(g_i)U(g_j)U(g_i)^\dagger U(g_j)^\dagger = \exp(i\phi)$. The non-trivial commutation relations require that the irreducible representations have dimensions larger than one which yields degeneracies in the spectrum of ρ^L and (ρ^R). For example, if $\phi = \pi$ (which is the case in the Haldane phase), then the spectrum is doubly degenerate, since ρ^L and ρ^R commute with the two unitary matrices U_x, U_z which anti-commute among themselves.

4.2 Extraction of projective representations from the mixed transfer matrix

The existence of degeneracies in the entanglement spectrum is a necessary condition for non-trivial cohomology classes. However, this does not distinguish among various non-trivial topological states (when there is more than one). Let us now show how to directly obtain the projective representations $U(g)$ with $g \in G$ for a given infinite MPS state.

As we learned in the preceding sections, the matrices $U(g)$ tell us how the Schmidt states transform under the symmetry operation g. Thus we can obtain all (projective) representations from the overlap of the Schmidt states with its symmetry transformed partners by

$$U_{\beta\beta'}(g) = \langle\beta|_R \left(\bigotimes_j u_j(g) |\beta'\rangle_R \right),$$

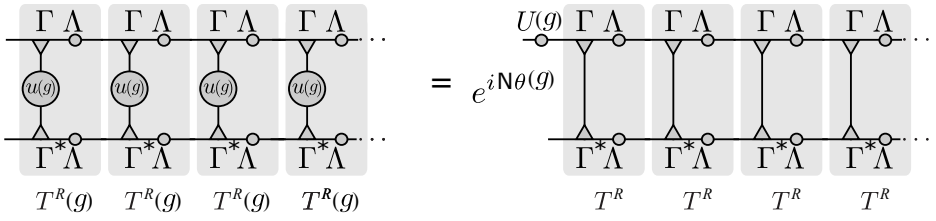

Fig. 4.1 Overlap of Schmidt states $|\alpha\rangle_R$ with its symmetry transformed partners. If the chain is assumed to be very long, the overlap can be expressed in terms of the eigenvector X corresponding the largest magnitude eigenvector $|\eta| = 1$ of the mixed transfer matrix (filled grey circles). The right boundary yields an overall phase factor $\exp iN\theta(g)$ which we ignore here (see text for details).

where $u_j(g)$ are the linear onsite representations and $|\beta\rangle_R$ the Schmidt states describing the right half chain. This overlap, represented in terms of an MPS in the canonical form is shown in Fig. 4.1. In particular, it corresponds to multiplying infinitely many mixed transfer matrices $T^R(g)$ and hence only the dominant eigenvector $X_{\beta\beta'}$ remains. Clearly, as the state is symmetric under g, the dominant eigenvalue η of the generalized transfer matrix $T^R(g)$ is of modulus one. On the other hand, we can apply the transformation Eq. (3.4) to each transformed matrix and see that only the $U(g)$ at the left end remains. Thus we can read off that

$$U_{\beta\beta'}(g) = X_{\beta\beta'}. \tag{4.1}$$

Here we normalize X such that $XX^\dagger = \mathbb{1}$ and ignore a constant phase factor which results from the right end. Thus the $U(g)$ matrices can be obtained by simply finding the dominant eigenvector of the mixed transfer matrix $T^R(g)$. Note that if the infinite MPS is not obtained in the canonical form, we need to multiply the RHS by the inverse of the eigenstate of the transfer matrix. Once we have obtained the $U(g)$ of each symmetry operation $g \in G$, we can read off the factor set and hence determine in which SPT the state is. In a similar way, SPTs stabilized by time reversal or inversion symmetry can be determined (see [50] for more details).

A useful procedure to detect SPT phases numerically from microscopic Hamiltonian is to first use the iTEBD or iDMRG algorithm to find the infinite MPS representation of the ground state. The projective representations of the symmetries and thus the characterizing factor set can be obtained by diagonalizing the mixed transfer matrices. This procedure is demonstrated by a simple Python program [51].

4.3 String order parameters

The method demonstrated above is very useful to detect SPT phases using MPS based algorithms. It is, however, not practical for Monte Carlo simulations or in any

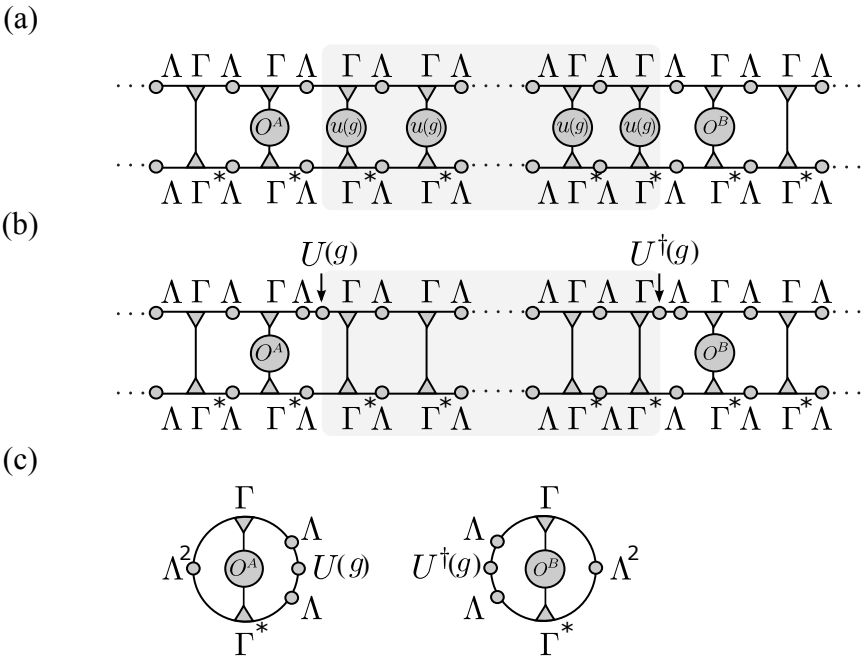

Fig. 4.2 Diagrammatic derivation of the string order $\mathcal{S}$ for a wave function which is symmetric under an internal transformation g and represented by an MPS in canonical form. (a): String order involving a segment of transformed sites terminated by operators O^A and O^B. (b): The matrices Γ_j transform according to Eq. (3.4) and all matrices U and $U^\dagger$ vanish except the ones at the edges (c): Using the properties of the transfer matrices (defined in the text), the expectation value in can be simplified for long segments.

experimental setup. For this we will show in this section how to derive non-local order parameter that detect SPT.

Perez-Garcia et al. [44] showed that the string order parameter, which was originally defined for $Z_2 \times Z_2$ symmetric spin chains [52]

$$\mathcal{S}^\alpha_{\mathrm{str}} \equiv \lim_{|j-k|\to\infty} \langle\psi_0|S^\alpha_j e^{i\pi \sum_{j\le l<k} S^\alpha_l} S^\alpha_k|\psi_0\rangle$$

can be generalized for systems with other symmetry groups. The generalized form for a state which is invariant under symmetry operations $u(g)$ reads:

$$\mathcal{S}(g, O^A, O^B) = \lim_{\ell\to\infty} \left\langle \psi_0 \middle| O^A(1) \left(\prod_{j=2}^{\ell-1} u_j(g) \right) O^B(\ell) \middle| \psi_0 \right\rangle . \tag{4.2}$$

The non-vanishing of this expression for generic operators only means that the state is symmetric, but does not distinguish among topologically distinct states. For example,

the Z_2 symmetric Ising paramagnet Eq. (2.4) has a non-vanishing string order with $O^A = O^B = \mathbb{1}$ and $u(g) = \sigma_x$ even though it does not represent any non-trivial SPT! Nevertheless, we will now show that if the operators $O^A(1), O^B(n)$ are chosen appropriately, this order parameter can distinguish certain topological states. Beside the necessary condition of the state being symmetric under g, there is a second more refined condition for when the string order is nonzero, which *can* distinguish them. For example, the string order defined by $O^A = O^B = S^z$ vanishes in the large D phase. Why does this occur even though the state is symmetric?

We will now closely follow a discussion given in Ref. [50] and show that Eq. (4.2) can distinguish certain SPT because of a *selection rule*. Intuitively, the string order corresponds to calculating the overlap between the wave function with g applied to ℓ consecutive sites and the wave function itself. Since g is a symmetry of the wave function, it does not change anything in the bulk of this segment and the overlap should not vanish. A diagrammatic representation of the string order is given in Fig. 4.2(a). If we represent the symmetry that is sandwiched in the middle using Eq. (3.4) and ignore the overall phase factor $e^{i\ell\theta}$, we obtain the expression that diagrammatically represented in Fig. 4.2(b). If ℓ is large, the part in between the $U(g)$ and $U^\dagger(g)$ is a product of orthogonal Schmidt states of the segment yielding a product of delta functions $\delta_{\alpha\alpha'}$ on the left and $\delta_{\beta\beta'}$ on the right [compare Fig. 4.2(c)]. That is, the string order is equal to the product

$$\mathcal{S}(g, O^A, O^B) = \left[\text{tr } (\Lambda \bar{O}^A \Lambda U(g))\right] \left[\text{tr } (\Lambda \bar{O}^B \Lambda U^*(g))\right], \tag{4.3}$$

where

$$\bar{O}^A_{\beta\beta'} = \sum_\alpha T^L_{\alpha\alpha;\beta\beta'}(O^A) \text{ and } \bar{O}^B_{\alpha'\alpha} = \sum_\beta T^R_{\alpha\alpha';\beta\beta'}(O^B) \tag{4.4}$$

with the generalized transfer matrices as defined in Eq. (3.2). The product Eq. (4.3) is nonzero unless at least one of the two factors is equal to zero. Whether the factors vanish depends on the symmetry of the operators $O^A(1), O^B(n)$ and can be seen as a selection rule for string order. Such selection rules exist only in the presence of additional symmetry. Thus, suppose that there are two symmetry operations g_j and g_k which commute but $U(g_j)U(g_k)U^\dagger(g_j)U^\dagger(g_j) = e^{i\phi}$. We consider the string correlator $\mathcal{S}(g_j, O^A, O^B)$, and focus on the left end of the interval. The operator O^A can be chosen to have a particular quantum number under g_k, i.e., $u(g_k)O^A u^\dagger(g_k) = e^{i\sigma}O^A$. Then a short calculation shows that $\bar{O}^A$ transforms in the same way under $U(g_j)$, i.e., $U(g_j)\bar{O}^A U^\dagger(g_j) = e^{i\sigma}\bar{O}^A$. It follows that

$$\begin{aligned} \text{tr } \left(\Lambda \bar{O}^A \Lambda U^\dagger(g_j)\right) &= \text{tr } \left(U(g_k)\Lambda \bar{O}^A \Lambda U^\dagger(g_j) U^\dagger(g_k)\right) \\ &= e^{i(\sigma-\phi)} \text{tr } \Lambda \bar{O}^A \Lambda U^\dagger(g_j). \end{aligned} \tag{4.5}$$

Thus we obtain a string order selection rule: the string order parameter vanishes if $\sigma \neq \phi$. Without the second symmetry Σ^b, the string order would not vanish. Hence a nonzero string order in a state (though intuitively surprising) is actually not so unusual; it is the *vanishing* of a string order that is the signature of a topological phase. Note that the string order might accidentally vanish (or become very small) at

some points even in a phase where $\sigma = \phi$. In that case one would have to find different operators O^A/O^B to distinguish the phases.

Note that the string order is not general in that there are SPT phases that cannot be detected by this approach. First, there are SPT protected by non-onsite symmetries for which this approach obviously fails. Second, more complex onsite symmetries exist which cannot be detected using simple string order parameters. Non-local order parameters that can detect avery possible SPT can be found in Ref. [50].

The string order for the spin-1 Heisenberg chain can, for example, be derived simply in this way. Consider the Heisenberg chain with the symmetries $\mathcal{R}^x = \exp(i\pi S^x)$ and $\mathcal{R}^z = \exp(i\pi S^z)$. Then the selection rule implies that the string order vanishes in the trivial phase if one of the operators O^A, O^B is odd under π rotations about the x axis. The string order vanishes in the nontrivial phase if one of these operators is *even* (since U^z is odd under flips about the x-axis in this phase). Thus the string order $\mathcal{S}(R_z, \mathbb{1}, \mathbb{1})$ vanishes in the nontrivial ($\phi = \pi$) phase and $\mathcal{S}(R_z, S_z, S_z)$ does not, while the situation is reversed in the trivial ($\phi = 0$) phase. It is a nice exercise to derive the value of the string order for the AKLT state which is known to be $\mathcal{S}(R_z, S_z, S_z) = 0.444444$.

5
Summary

In these lecture notes, we first introduced some basic concepts of entanglement and discussed the area law for gapped ground states in 1D. We then derived the MPS representation and showed that these describe 1D ground states efficiently. Starting from the MPS transformation operations, we introduced the concept of SPT phases. Using an intuitive approach by studying the symmetry transformations of a segment of consecutive site, we demonstrated the stability of SPT phases. Finally, we proposed methods to detect SPT phases in numerical simulations.

While we discussed here only bosonic SPT in 1D, there exists a large number of generalizations. For example, based on the fractionalization of symmetry operators, the classification can be extended to fermionic models. Using the concept of symmetry fractionalization, it can for example be shown that the $\mathbb{Z}$ classification of 1D topological superconductors breaks down to $\mathbb{Z}_8$ in the presence of interaction [53, 54]. Recently there has been significant advance in understanding SPT phases in higher dimensions. In particular it has been shown that SPT phases in higher dimensions can be classified by higher order co-cycles $H^n(G, U(1))$ [10].

References

[1] L. D. Landau. *Phys. Z. Sowjetunion*, 11:26, 1937.

[2] X.-G. Wen. *Phys. Rev. B*, 40:7387, 1989.

[3] F. Verstraete, J. I. Cirac, J. I. Latorre, E. Rico, and M. M. Wolf. Renormalization-group transformations on quantum states. *Phys. Rev. Lett.*, 94:140601, Apr 2005.

[4] Xie Chen, Zheng-Cheng Gu, and Xiao-Gang Wen. Local unitary transformation, long-range quantum entanglement, wave function renormalization, and topological order. *Phys. Rev. B*, 82:155138, Oct 2010.

[5] Zheng-Cheng Gu and Xiao-Gang Wen. Tensor-entanglement-filtering renormalization approach and symmetry-protected topological order. *Phys. Rev. B*, 80:155131, Oct 2009.

[6] Frank Pollmann, Ari M. Turner, Erez Berg, and Masaki Oshikawa. Entanglement spectrum of a topological phase in one dimension. *Phys. Rev. B*, 81:064439, Feb 2010.

[7] Xie Chen, Zheng-Cheng Gu, and Xiao-Gang Wen. Classification of gapped symmetric phases in one-dimensional spin systems. *Phys. Rev. B*, 83:035107, Jan 2011.

[8] Xie Chen, Zheng-Cheng Gu, and Xiao-Gang Wen. Complete classification of one-dimensional gapped quantum phases in interacting spin systems. *Phys. Rev. B*, 84:235128, Dec 2011.

[9] Schuch, N. and Pérez-García, D. and Cirac, J. I. Classifying quantum phases using matrix product states and projected entangled pair states. *Phys. Rev. B*, 84:165139, Oct 2011.

[10] Xie Chen, Zheng-Cheng Gu, Zheng-Xin Liu, and Xiao-Gang Wen. Symmetry protected topological orders and the group cohomology of their symmetry group. *Phys. Rev. B*, 87:155114, Apr 2013.

[11] C. L. Kane and E. J. Mele. Z2 topological order and the quantum spin hall effect. *Phys. Rev. Lett.*, 95:146802, Sep 2005.

[12] A. Kitaev. Periodic table for topological insulators and superconductors. 2009.

[13] Andreas P. Schnyder, Shinsei Ryu, Akira Furusaki, and Andreas W. W. Ludwig. Classification of topological insulators and superconductors in three spatial dimensions. *Phys. Rev. B*, 78(19):195125, Nov 2008.

[14] F. D. M. Haldane. Continuum dynamics of the 1-d heisenberg antiferromagnet: Identification with the o(3) nonlinear sigma model. *Phys. Lett. A*, 93(9):464 – 468, 1983.

[15] Ian Affleck, Tom Kennedy, Elliott H. Lieb, and Hal Tasaki. Rigorous results on valence-bond ground states in antiferromagnets. *Phys. Rev. Lett.*, 59:799–802, Aug 1987.

[16] F. D. M. Haldane. Nonlinear field theory of large-spin heisenberg antiferromag-

nets: Semiclassically quantized solitons of the one-dimensional easy-axis néel state. *Phys. Rev. Lett.*, 50:1153, 1983.

[17] Marcel den Nijs and Koos Rommelse. Preroughening transitions in crystal surfaces and valence-bond phases in quantum spin chains. *Phys. Rev. B*, 40:4709–4734, Sep 1989.

[18] Hal Tasaki. Quantum liquid in antiferromagnetic chains: A stochastic geometric approach to the haldane gap. *Phys. Rev. Lett.*, 66:798–801, Feb 1991.

[19] Wei Chen, Kazuo Hida, and B. C. Sanctuary. Ground-state phase diagram of $s = 1$ XXZ chains with uniaxial single-ion-type anisotropy. *Phys. Rev. B*, 67:104401, Mar 2003.

[20] Pasquale Calabrese and John Cardy. Entanglement entropy and quantum field theory. *J. Stat. Mech.*, 2004(06):P06002, 2004.

[21] L. Tagliacozzo, T. R. de Oliviera, S. Iblisdir, and J. I. Latorre. Scaling of entanglement support for matrix product states. *Phys. Rev. B*, 78:024410, 2008.

[22] P. Calabrese and A. Lefevre. Entanglement spectrum in one-dimensional systems. *Phys. Rev. A*, 78(032329):032329, 2008.

[23] Frank Pollmann, Subroto Mukerjee, Ari A. M. Turner, and Joel E. Moore. Theory of finite-entanglement scaling at one-dimensional quantum critical points. *Phys. Rev. Lett.*, 102(25):255701, 2009.

[24] Michael Levin and Xiao-Gang Wen. Detecting topological order in a ground state wave function. *Phys. Rev. Lett.*, 96(11):110405, 2006.

[25] Alexei Kitaev and John Preskill. Topological entanglement entropy. *Phys. Rev. Lett.*, 96(11):110404, 2006.

[26] F. Verstraete, J.I. Cirac, and V. Murg. Matrix product states, projected entangled pair states, and variational renormalization group methods for quantum spin systems. *Adv. Phys.*, 57:143, 2008.

[27] Ulrich Schollwöck. The density-matrix renormalization group in the age of matrix product states. *Ann. Phys.*, 326(1):96 – 192, 2011.

[28] H. Li and F. D. M. Haldane. Entanglement spectrum as a generalization of entanglement entropy: Identification of topological order in non-abelian fractional quantum hall effect states. *Phys. Rev. Lett.*, 101:010504, 2008.

[29] Don Page. Average entropy of a subsystem. *Phys. Rev. Lett.*, 71(9):1291–1294, August 1993.

[30] J Eisert, M Cramer, and M B Plenio. Colloquium: Area laws for the entanglement entropy. *Rev. Mod. Phys.*, 82(1):277–306, February 2010.

[31] M. B. Hastings. An area law for one-dimensional quantum systems. *J. Stat. Mech.*, P08024(08), 2007.

[32] M. Fannes, B. Nachtergaele, and R. F. Werner. Finitely correlated states on quantum spin chains. *Comm. Math. Phys.*, 144(3):443–490, 1992.

[33] Stellan Östlund and Stefan Rommer. Thermodynamic limit of density matrix renormalization. *Phys. Rev. Lett.*, 75:3537–3540, Nov 1995.

[34] Stefan Rommer and Stellan Östlund. Class of ansatz wave functions for one-dimensional spin systems and their relation to the density matrix renormalization group. *Phys. Rev. B*, 55:2164–2181, Jan 1997.

[35] Daniel Gottesman and M B Hastings. Entanglement versus gap for one-dimensional spin systems. *New J. Phys.*, 12(2):025002, 2010.
[36] N. Schuch, M. M. Wolf, F. Verstraete, and J. I. Cirac. Entropy scaling and simulability by matrix product states. *Phys. Rev. Lett.*, 100(3):030504, 2008.
[37] G. Vidal, J. I. Latorre, E. Rico, and A. Kitaev. Entanglement in quantum critical phenomena. *Phys. Rev. Lett.*, 90(22):227902, Jun 2003.
[38] G. Vidal. Classical simulation of infinite-size quantum lattice systems in one spatial dimension. *Phys. Rev. Lett.*, 98(070201):070201, FEB 16 2007.
[39] R. Orús and G. Vidal. Infinite time-evolving block decimation algorithm beyond unitary evolution. *Phys. Rev. B*, 78:155117, Oct 2008.
[40] D. Perez-Garcia, F. Verstraete, M.M. Wolf, and J.I. Cirac. Matrix product state representations. *Quantum Inf. Comput.*, 7:401, 2007.
[41] Ian P McCulloch. From density-matrix renormalization group to matrix product states. *J. Stat. Mech.*, P10014(10), 2007.
[42] Jonas A. Kjäll, Michael P. Zaletel, Roger S. K. Mong, Jens H. Bardarson, and Frank Pollmann. Phase diagram of the anisotropic spin-2 xxz model: Infinite-system density matrix renormalization group study. *Phys. Rev. B*, 87:235106, Jun 2013.
[43] I. Affleck, T. Kennedy, E. Lieh, and H. Tasaki. *Phys. Rev. Lett.*, 59:799, 1988.
[44] D. Perez-Garcia, M. M. Wolf, M. Sanz, F. Verstraete, and J. I. Cirac. String order and symmetries in quantum spin lattices. *Phys. Rev. Lett.*, 100:167202, Apr 2008.
[45] F. Pollmann, A. M. Turner, E. Berg, and M. Oshikawa. Entanglement spectrum of a topological phase in one dimension. *Phys. Rev. B*, 81:064439, 2010.
[46] G. Karpilovsky. *The Schur multiplier*. LMS monographs. Clarendon Press, 1987.
[47] Frank Pollmann, Erez Berg, Ari M. Turner, and Masaki Oshikawa. Symmetry protection of topological phases in one-dimensional quantum spin systems. *Phys. Rev. B*, 85:075125, Feb 2012.
[48] F. Anfuso and A. Rosch. Fragility of string orders. *Phys. Rev. B*, 76:085124, 2007.
[49] Z-C. Gu and X-G. Wen. Tensor-entanglement-filtering renormalization approach and symmetry protected topological order. *Phys. Rev. B*, 80:155131, 2009.
[50] Frank Pollmann and Ari M. Turner. Detection of symmetry-protected topological phases in one dimension. *Phys. Rev. B*, 86:125441, Sep 2012.
[51] Frank Pollmann. Python code of an mps based simulation, demonstrating how to detect spt phases. http://www.pks.mpg.de/ frankp/code/spt.py.
[52] Marcel den Nijs and Koos Rommelse. Preroughening transitions in crystal surfaces and valence-bond phases in quantum spin chains. *Phys. Rev. B*, 40(7):4709–4734, Sep 1989.
[53] Lukasz Fidkowski and Alexei Kitaev. Effects of interactions on the topological classification of free fermion systems. *Phys. Rev. B*, 81:134509, Apr 2010.
[54] Ari M. Turner, Frank Pollmann, and Erez Berg. Topological phases of one-dimensional fermions: An entanglement point of view. *Phys. Rev. B*, 83:075102, Feb 2011.